Histol Histopathol (2009) 24: 283-292
DOI: 10.14670/HH-24.283

http://www.hh.um.es

Histology and Histopathology
Cellular and Molecular Biology

Intestinal uptake of amyloid ß protein through columnar epithelial cells in suckling mice

Yasuhisa Ano[1], Hiroyuki Nakayama[2,4], Akikazu Sakudo[5], Yoriko Sawano[3], Masaru Tanokura[3], Shigeyoshi Itohara[6] and Takashi Onodera[1,4]

[1]Department of Molecular Immunology, [2]Department of Veterinary Pathology, [3]Department of Food Biotechnology and [4]Research Center for Food Safety, Graduate School of Agricultural and Life Sciences, the University of Tokyo, Yayoi, Bunkyo-ku, Tokyo, Japan, [5]Research Institute for Microbial Diseases, Osaka University, Yamadaoka, Suita, Osaka , Japan and [6]Laboratory for Behavioral Genetics, Brain Science Institute, RIKEN, Wako, Saitama, Japan

Summary. The mechanism of transmission of amyloid protein, especially the dynamics in the intestine, is still largely unknown. In the present study, a fusion protein (Aß-EGFP) that combined enhanced green fluorescent protein with amyloid-ß protein (Aß) was orally administered to mice before and after weaning, and the uptake and kinetics of amyloid protein within the intestine were elucidated through histopathology. Aß-EGFP was incorporated into the cytoplasm of columnar epithelial cells, rather than M cells, at 3 h after administration and thereafter. Aß-EGFP then accumulated in the crypt, Peyer's patch, and even the spleen. However, this uptake was not observed in weaned mice. These results suggest that a specific tolerant mechanism for incorporation of Aß escaped from the digestion exists during suckling periods. This age-dependent uptake is important for estimating the risk of transmission.

Key words: Amyloid-ß protein, Amyloidoses, Columnar epithelial cells, Suckling periods, Uptake

Introduction

Amyloidoses are characterized by tissue dysfunction caused by the deposition of insoluble and abnormal ß-sheet structures of proteins, known as amyloid fibrils, which consequently mold highly stable products (Westermark, 1998). Amyloid fibrils are notably resistant to enzymatic degradation by proteases. To date, more than 20 amyloid proteins, such as prion protein and amyloid ß protein, have been identified (Xing and Higuchi, 2002).

Recent reports have demonstrated that orally inoculated ApoAII protein (Johan et al., 1998; Xing and Higuchi, 2001; Cui et al., 2002) and intracerebrally inoculated amyloid ß protein (Melanie and Mathias, 2006; Riek, 2006) induced systemic and cerebral amyloidoses, respectively. It is assumed that the common mechanism of uptake relies on aggregated proteins, such as amyloid, which are resistant to proteases due to reports of oral transmission of amyloid protein. However, the uptake and subsequent kinetics, especially in intestine of these transmissible amyloid proteins, are still largely unknown.

Suckling cows are thought to have the highest risk during the weaning period for infection by PrP^{Sc}, which has been shown to contaminate foods by statistical analysis (Arnold and Wilesmith, 2004). During suckling, the intestinal epithelium is tolerant for transmission of proteins that allow uptake of immunogloblins and growth factors in breast milk. Therefore, the intestinal epithelium is thought to play an important role in the transmission of amyloid protein through the intestinal barrier.

The present study elucidated the age-dependent mechanism of uptake and internal distribution of amyloid, protein via the peroral route. A fusion protein of amyloid ß protein that was abundant in a ß sheet structure with a fluorescent protein (EGFP) were orally administrated into suckling and adult mice and then analyzed by fluorescent imaging.

Offprint requests to: Professor Dr. H. Nakayama, Department of Veterinary Pathology, Graduate School of Agricultural and Life Sciences, The University of Tokyo, Bunkyo-ku, Tokyo 113-8657, Japan. e-mail: anakaya@mail.ecc.u-tokyo.ac.jp

Materials and methods

Experimental animals

Five-day-old, 10-day-old, 15-day-old, 20-day-old and 25-day-old ICR mice (Japan SLC, Shizuoka, Japan) were housed in SPF conditions in an alternating 14/10-h light/ dark cycle. Animals were given free access to standard laboratory food (Japan CLEA, Tokyo, Japan) and tap water. Animals were treated according to procedures authorized by the Animal Experiment Committee of the Faculty of Agriculture, University of Tokyo.

Preparation of fusion protein

A fusion protein (Aß-EGFP) of the murine ß amyloid protein (Aß, 42 amino acids) at the N-terminal and the enhanced green fluorescent protein (EGFP, 238 amino acids) at the C-terminal was mass-produced by the following method. Aß-EGFP was derived from a fusion of the Aß gene with the EGFP gene. Aß-EGFP containing polymerase chain reaction (PCR) products was cloned into a pROX1-vector and subsequently constructed as the Aß-EGFP-expressing plasmid pROX1-Aß-EGFP. *E. coli* BL21 (DE3) Rosetta II was transformed by pROX1-Aß-EGFP. The pROX1-Aß-EGFP-harboring *E. Coli* were incubated in SB medium supplemented with ampicillin at 20°C for 18 h after 1mM IPTG induction. Cells were harvested by centrifugation at 5,000xg for 10 min at 4°C. The supernatant was removed and sonicated in phosphate-buffered saline (PBS) on ice. The precipitated fraction of the cell lysate was collected by centrifugation at 18,000xg for 10 min at 4°C before the pellet was washed with PBS containing 0.4 % Triton X-100 with shaking for 30 min at 4°C. After three repetitions of the centrifugation/washing procedures, the resultant pellet fraction was stored at -20°C. The Aß-EGFP concentration was determined by comparing CBB staining data after SDS-PAGE with known quantities of bovine serum albumin (BSA; Sigma, St. Louis, MO, USA). 3.6 mg of Aß-EGFP was therefore obtained from 200 ml of culture medium. The remaining culture media were used for secondary structure analysis and oral administration.

Secondary structure analysis

Attenuated total reflection (ATR) fourier-transformed (FT)-infrared (IR) spectra (600-4000 cm^{-1}) were collected by an FT-IR spectrophotometer (Nicolet 6700; Thermo Fisher Scientific K.K., Waltham, MA, USA) with ATR equipment-containing a ZnSe ATR crystal, an ETC-Ever-Glo IR source, a deuterated lanthanum triglycine sulfate (DLATGS) detector, and a KBr beam-splitter under purging with a continuous flow of dried air. (Air Tech Japan Ltd., Tokyo, Japan). The α-helix, ß-sheet, ß-turn, and random coil contents of murine Aß-EGFP were estimated from the amide-I region of ATR IR spectra with ATR corrections as follows. Briefly, peaks of the amide-I region were first treated by Fourier self-deconvolution and then curve-fitted using the Gauss and Lorentz formulae with OMNIC. The area corresponding to each secondary structure was calculated accordingly (Bradley and Nishida, 2005) and expressed as a percentage of the sum of the areas measured by X-ray structure analysis (Hering et al., 2002).

Administration of Aß-EGFP, and preparation of tissue specimens

To observe time-dependent uptake, ICR suckling mice (age: 10 days) were orally administered 150 μl of Aß-EGFP (4.2 mg/ml), a microsphere with albumin green fluorescence (4.2 mg/ml) (Albumin-Fluor; MPT, Rostock, Germany) diluted with PBS (pH 7.4). This process was defined as (A). At 0, 3, 6 h, and 1 and 4 days postadministration (p.a.), mice (n=3 animals per point in time) were euthanized with ether. The intestines, liver and spleen were removed and fixed by immersion in PBS containing 4% paraformaldehyde for 2 h before being washed in PBS containing 6.8 % sucrose. After dehydration in 100% acetone for 1 h, tissue samples were embedded in a resin (Technovit 8100; Heraeus Kulzer, Wehrheim, Germany) according to the manufacturer's instructions at a thickness of 4 μm. Sections were mounted on silanized slide glasses and observed under fluorescent microscopy (OLYMPUS, Tokyo, Japan).

To examine the internal dynamics at the early stage of uptake, suckling mice (age: 10 days and n = 3 animals per sample) were continuously administered with 150 μl of Aß-EGFP (4.2 mg/ml) or PBS alone for 6 doses at 2-h intervals. Twelve hours after the last administration, another 6-dose regimen was repeated. This process was defined as (B). Before the observations, sections were stained with DAPI.

In addition to observing the difference of uptake between suckling periods and weaning periods, mice (age: 10, 15, 20, 25 days and n=3) were administered with Aß-EGFP (4.2 mg/ml). At 3 h p.a. mice were euthanized with ether. Mice used were weaned at 18-day-old. The amount of administration was 100μl in 15-day-old mice and in proportion of weight of 15, 20 and 25-day-old mice to that of 10-day-old mice. This procedure was defined as (C).

Otherwise, to examine further kinetics after uptake, suckling mice (age: 5 days and n=3) were continuously administered with 150 μl of Aß-EGFP (4.2 mg/ml) for 3 doses at 3 h intervals. This inoculation was repeated from 5 to 19 days of age. In total, 45 administrations (28.3 mg of Aß-EGFP) were performed. This procedure was defined as (D). After these treatments, experimental animals were then euthanized. The same procedures were repeated for the tissue preparations as described above.

These administration procedures were summarized in Table 1.

Quantification of green fluorescence was carried out using the Image J program (developed at the US National Institutes of Health and available on the internet at http://rsbweb.nih.gov/ij/) on a Windows computer. Statistical analysis between groups ($p<0.01$) were performed by Student's t-test.

Identification of Aß-EGFP

Aß-EGFP was identified by immunohistochemistry. Sections obtained from mice treated by (B), (C) and (D) for Aß-EGFP were pretreated with 0.1% $CaCl_2$ pH 7.8 containing 0.01% trypsin for 10 min at 37°C and then quenched in 0.3% hydrogen peroxide in methanol for 30 min. After incubation with the rabbit anti-living colors® full-length polyclonal antibody (1:200; Clontech, CA, USA) at 37°C for 2 h and secondary horseradish peroxidase-coupled goat anti-rabbit IgG antibody (4 μg/ml; Nichirei, Tokyo, Japan) at room temperature for 30 min, diamino benzidine (DAB; Wako, Osaka, Japan) was applied for 10 min. Sections were counterstained in hematoxylin for 1 min.

Lectin staining to identify the targeted cells

To analyze the cells incorporating Aß-EGFP, the resin sections of condition (b) were treated with PBS containing 1% BSA for 30 min. *Ulex europaeus* agglutinin (UEA-1) conjugated with rhodamine (Vector Labs, Burlingame, CA, USA) and wheat germ agglutinin (WGA) conjugated with Alexa fluor® 350 (Molecular Probes, Eugene, OR, USA) were used. The sections were reacted at room temperature for 1 h with the lectins (10 μg/ml).

Distribution of the peripheral nervous system in intestinal tissue

The peripheral nervous system of suckling mice was observed by indirect immunofluorescence. Sections treated with (B) and (D) were pretreated with 0.1% $CaCl_2$ pH 7.8 containing 0.01 % trypsin for 15 min at 37°C. After incubation with anti-PgP 9.5 polyclonal antibody (1:100; abcam, Tokyo, Japan) for 2 h at 37°C and secondary Alexa Fluor® 546 coupled goat anti-rabbit IgG (H+L) antibody (5 μg/ml; Molecular Probe, Eugene, OR, U.S.A.) at room temperature for 30 min, sections were observed under a fluorescent microscope with the appropriate filters.

Results

Mass production and second structure analysis of Aß-EGFP

A total of 840 mg of Aß-EGFP with 90% purity was produced as the result of repeated massive incubation of transfected *E. coli* with the fusion gene. The amide-I region of the ATR FT-IR spectra of Aß-EGFP was separated into 9 peaks by peak resolution analysis based on the Gauss and Lorentz formula (Fig. 1). These peaks revealed that the secondary structure of the Aß-EGFP product consisted of 0% α-helix, 45.9% ß-sheet, 33.4% ß-turn, and 20.7% random coil structures.

Time-dependent Incorporation

Aß-EGFP was detected in the villous epithelium of the intestines at 3 and 6 h p.a. (Fig. 2c,e). The incorporated Aß-EGFP, which assumed a fine granular shape, was broadly distributed in the cytoplasm (from the luminal to the interstitial side). Aß-EGFP was shifted

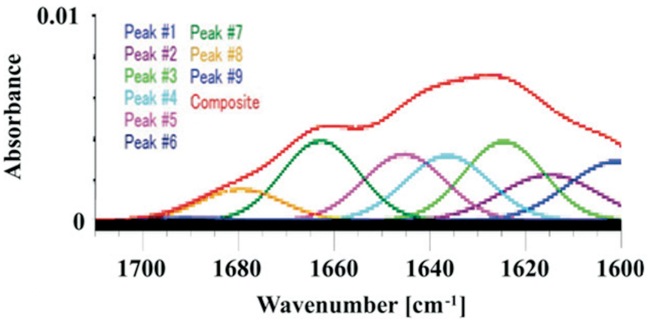

Fig. 1. Secondary structure analysis. The amide-I region of fourier-transformed (FT)-infrared (IR) spectra (composite) of Aß-EGFP were separated into 9 peaks (Peaks #1-9). The resolution of each peak was calculated by Fourier deconvolution and curve fitting based on the Gauss and Lorentz formulae. The ratio of area to composite represents the corresponding percentage of each structure; peaks #6 (α-helix), #1-4 and #8 (ß-sheet), #7 and #9 (ß-turn) and #5 (random coil) are indicated accordingly.

Table 1. Procedures performed in the present study.

Procedure	Age of animals at the first administration	Administration
(A)	10 days	Single dose
(B)	10 days	6 doses at 2-h intervals and another 6-doses administration after 12 h (total 12 doses)
(C)	10, 15, 20, 25 days	Single dose
(D)	5 days	3 doses at 3-h intervals from 5-day-old to 19-day-old (total 45 doses)

to the villous interstitium at 6 h p.a., and fluorescent granules gradually disappeared by 24 h p.a. (Fig. 2g,i). Albumin-Fluor was also detected in the villous epithelium at 3 (Fig. 2d) and 6 (Fig. 2f) h p.a., and thereafter shifted to the villous interstitium. Although Albumin-Fluor consists of microparticles under normal conditions, it was diffusively distributed in the epithelial cells without assuming a microparticulate appearance, particularly in the luminal portion of the cell where Aß-EGFP was detected as an aggregate. Analysis of the green fluorescent area showed that most green fluorescence was detected in the villi at 3 h p.a. (Fig. 2i).

Deposition in the crypt patch, Peyer´s patch and spleen

Immunohistchemistry using immuno-peroxidase confirmed the fluorescence data for conditions (B) and (D) (Fig. 3h). Condition (B) revealed that Aß-EGFP was detected in the villous interstitium and epithelium (Fig. 3d). Aß-EGFP was ubiquitously distributed in the cytoplasm of villous epithelial cells (concentrated especially at the luminal side). However, Aß-EGFP was not observed in the intercellular spaces (Fig. 3g). Besides the dome epithelial cells and subepithelial region of the Peyer's patch (Fig. 3e), Aß-EGFP was also detected in the epithelial cells and interstitium of the crypt (Fig. 3f). In condition (D), Aß-EGFP was significantly deposited in crypt patches (Fig. 4a and Fig. 7d) and distributed evenly in the splenic red pulp (Fig. 4b,c,e,f).

Age-dependent incorporation

Aß-EGFP was incorporated through the villous epithelium in 10 (Fig. 5 a,e) and 15 (Fig. 5 b,f)-day-old mice. On the other hand, Aß-EGFP was attached on the luminal surface of villous epithelial cells but scarcely incorporated into the villous columnar epithelial cells in 20-day-old (Fig. 5 c,g) mice and not incorporated in 25-day-old mice (Fig. 5 d,h). Aß-EGFP was also identified by immunohistochemistry for EGFP, but the sensitivity of the detection was lower than that of fluorescent Aß-EGFP.

Incorporation across absorptive epithelial cells

Four kinds of cells were identified in the intestinal villous epithelium of 10-day-old suckling mice: UEA-1-positive and WGA-negative (UEA-1+/WGA-) (orange), UEA-1-positive and WGA-positive (UEA-1+/WGA+) (pink), UEA-1-negative and WGA-positive (UEA-1-/WGA+) (blue), and UEA-1-negative and WGA-negative (UEA-1 - WGA+) cells. Aß-EGFP (Fig. 6b,d) were mainly detected in UEA-1-/WGA+ cells, but not in UEA-1+/WGA+ cells. In addition to these cells, UEA-1+/WGA- cells were identified in the dome epithelium of Peyer's patch, and Aß-EGFP were detected in these cells (Fig. 6 f,h).

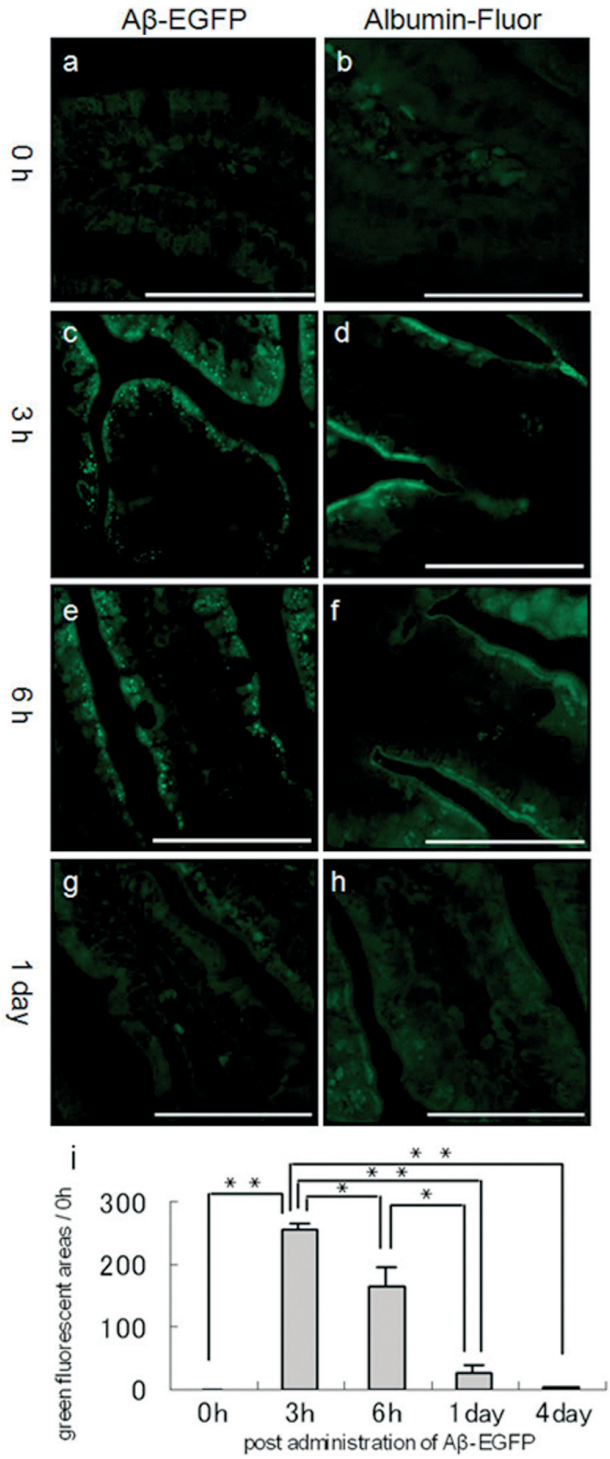

Fig. 2. Time-dependent uptake through villi. Villus epithelia of 10-day-old suckling mice orally administered **(a, c, e, g)** with Aß-EGFP and Albumin-Fluor **(b, d, f, h)** at 0 **(a, b)**, 3 **(c, d)**, 6 h **(e, f)**, and 1 **(g, h)** hour post-administration (p.a.). Aß-EGFP and Albumin-Fluor were incorporated into epithelial cells at 3 h p.a. Semiquantitative analysis of green fluorescent areas showed maximum signal at 3 h p.a.. Results are expressed as the mean ± s.d. Statistical differences were determined by Student's t-test. *P<0.05, **P<0.01 (i). Scale bar: 50 μm.

Distribution of the peripheral nervous system near the villus and crypt patches

Large amounts of peripheral nervous system cells and their plexus were distributed in the intestine of suckling mice. The peripheral nervous system very closely neighbored the epithelial cells incorporating (Fig. 7a) and the crypt patches deposited (Fig. 7b) with abundant Aß-EGFP.

Discussion

Secondary structure analysis suggests that the Aß-EGFP utilized in the present study was an amyloidotic protein with an abundant ß-sheet structure. This Aß-EGFP might not be degraded by gastric juices and intestinal enzymes because of its abundant stable ß-sheet structure. Aß-EGFP was incorporated by villous epithelial cells with its original shape. In contrast,

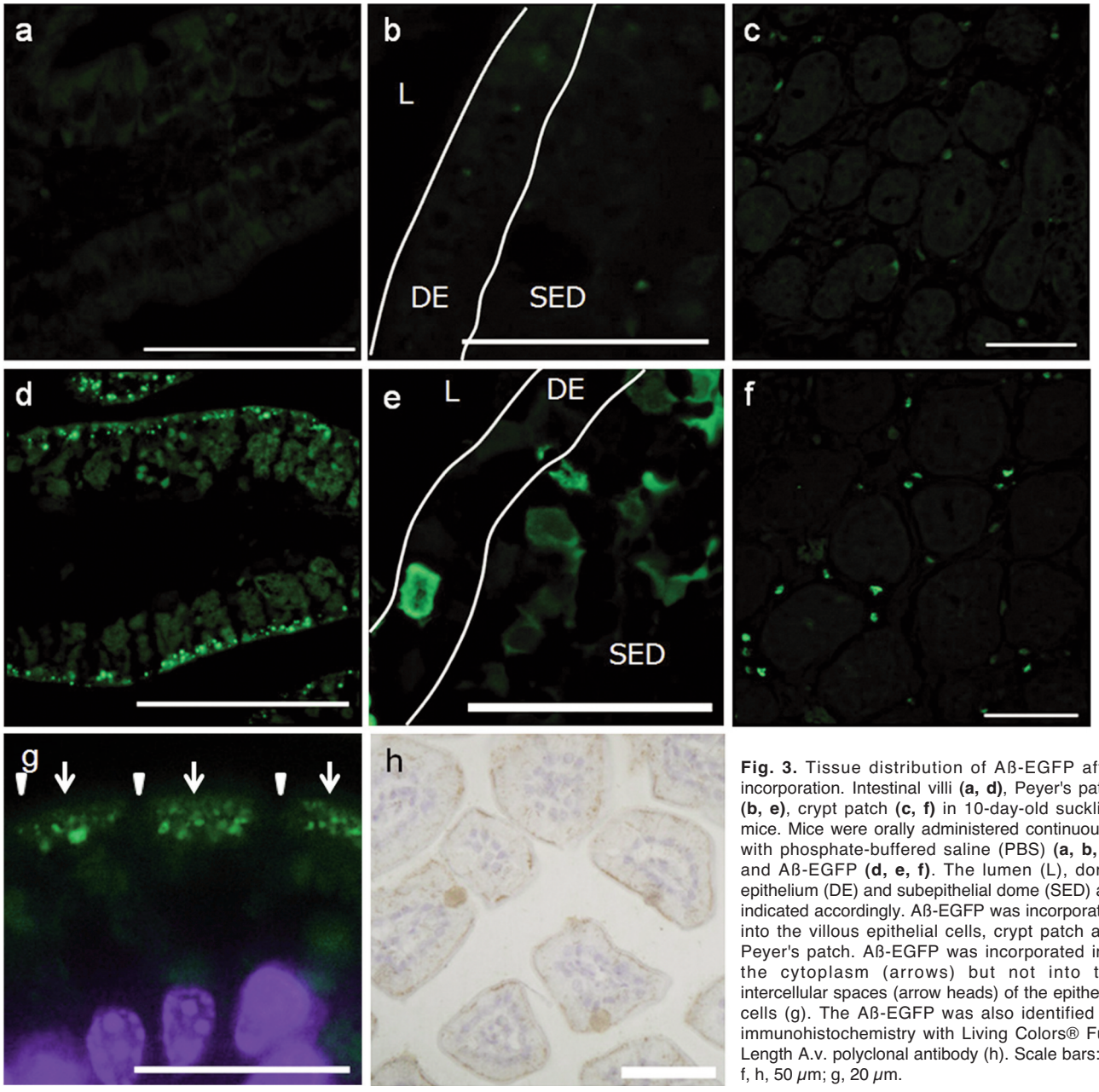

Fig. 3. Tissue distribution of Aß-EGFP after incorporation. Intestinal villi **(a, d)**, Peyer's patch **(b, e)**, crypt patch **(c, f)** in 10-day-old suckling mice. Mice were orally administered continuously with phosphate-buffered saline (PBS) **(a, b, c)** and Aß-EGFP **(d, e, f)**. The lumen (L), dome epithelium (DE) and subepithelial dome (SED) are indicated accordingly. Aß-EGFP was incorporated into the villous epithelial cells, crypt patch and Peyer's patch. Aß-EGFP was incorporated into the cytoplasm (arrows) but not into the intercellular spaces (arrow heads) of the epithelial cells (g). The Aß-EGFP was also identified by immunohistochemistry with Living Colors® Full-Length A.v. polyclonal antibody (h). Scale bars: a-f, h, 50 μm; g, 20 μm.

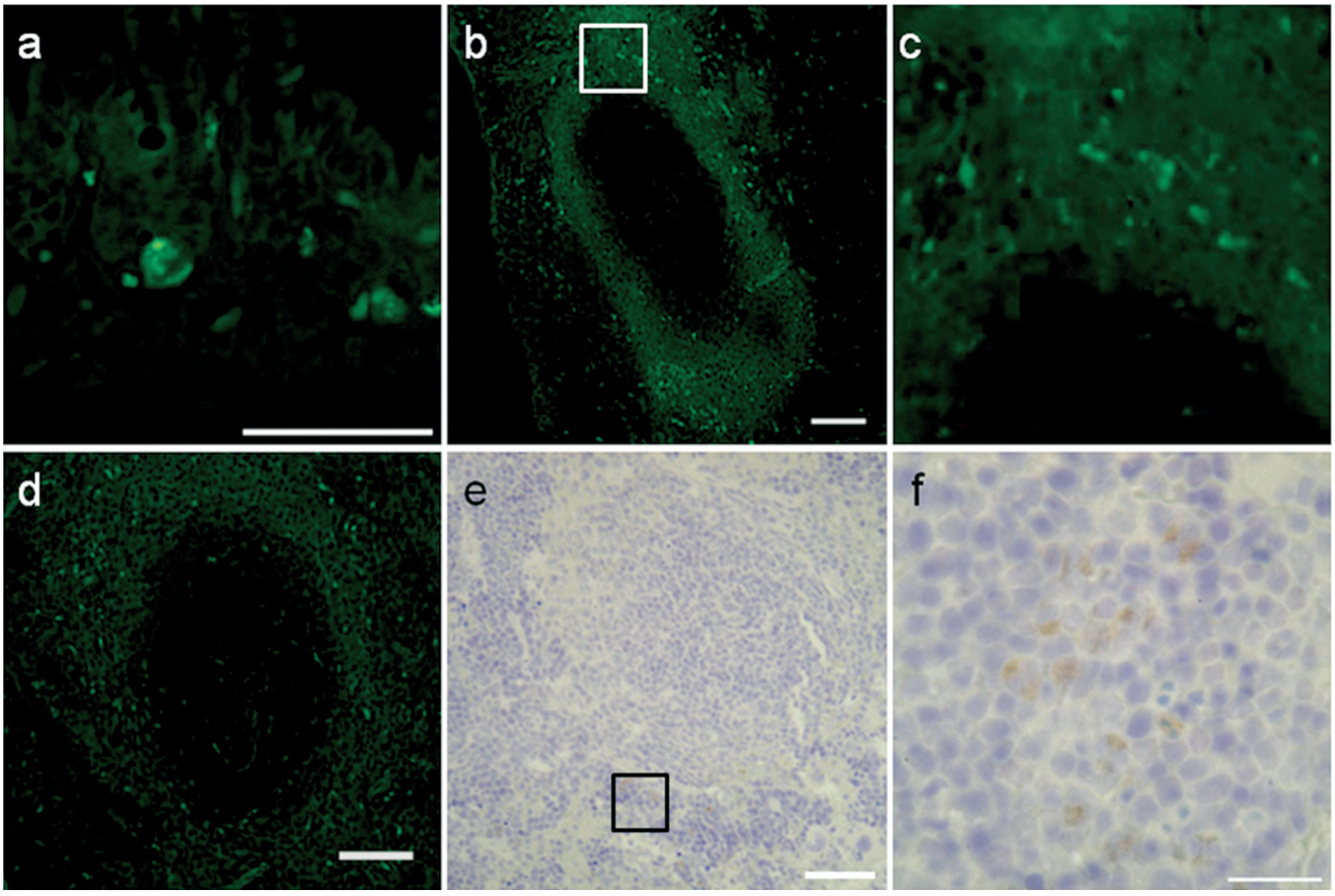

Fig. 4. Deposition of Aß-EGFP in crypt patches and spleen. Crypt patch **(a)**, and spleen **(b, c, d, e, f)**. Mice were orally administered continuously from 5 to 19 days of age with Aß-EGFP **(b, c, e, f)**, or given no treatment **(d)**. Immunohistoshemistry with Living Colors® Full-Length A.v. polyclonal antibody **(e, f)**. Aß-EGFP was deposited massively in crypt patches and distributed in splenic red pulp. Scale bars: a, b, d, e, 50 μm; f, 20 μm.

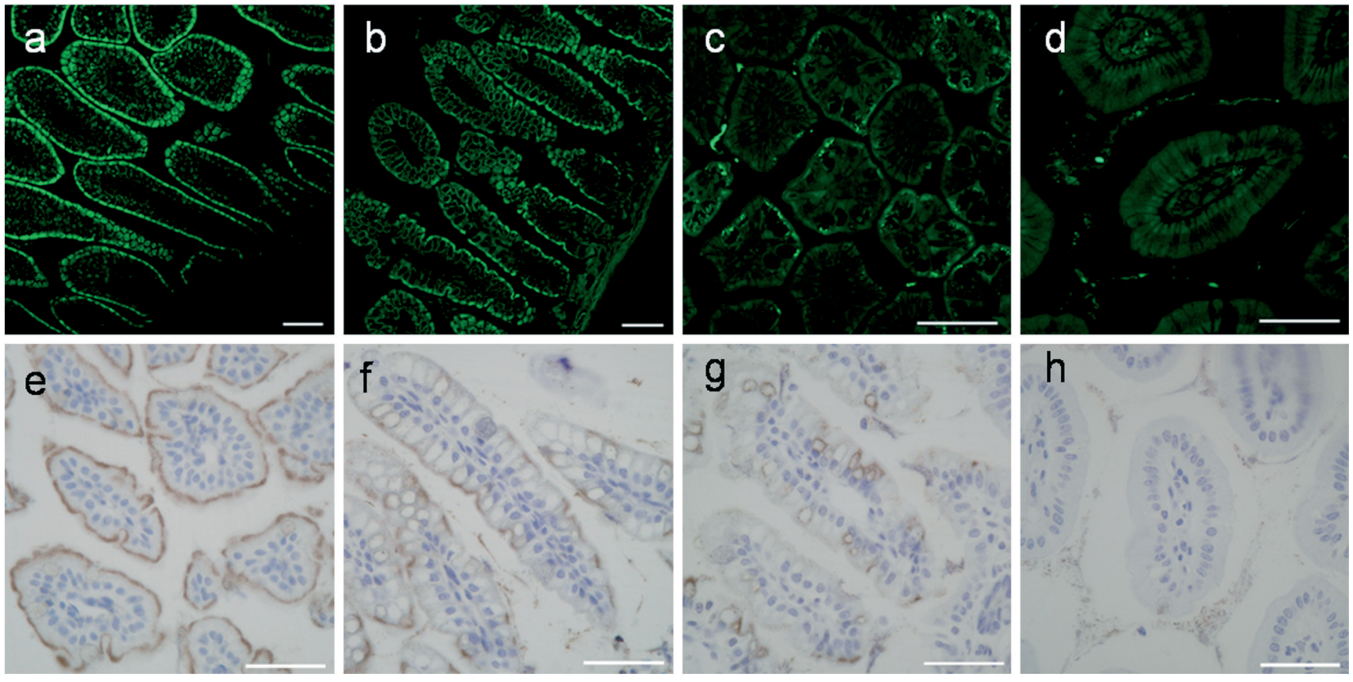

Fig. 5. Age-dependent uptake of Aß-EGFP. Intestinal villi of 10 **(a and e)**, 15 **(b and f),** 20 **(c and g)**, 25 (d and h)-day-old mice orally administered with Aß-EGFP. Aß-EGFP was detected in the cytoplasm of villous epithelial cells in 10 and 15-day-old but not 25-day-old mice. Scale bar: 50 μm.

Albumin-Fluor might have been digested in the stomach and then diffusively incorporated into the epithelial cells. Therefore, the proteins withstood the digestion of gastric juices and intestinal enzyme may be incorporated through the villous epithelial cells by a certain common mechanism.

Villous epithelial cells are composed of absorptive, goblet, endocrine, basal granular, and Paneth cells (Hunyady et al., 2002). Among murine intestinal epithelial cells, UEA-1+/WGA-, UEA-1-/WGA+, UEA-1-/WGA+ and UEA-1-/WGA- cells are the M (orange), goblet (pink), columnar (blue) and other cells (e.g. endocrine cells), respectively (Clark et al., 1993). Villous epithelium in 10-day-old suckling mice is composed of columnar, goblet, and other types of cells. The dome epithelium in Peyer's patches mostly consists of M cells. In the present experiment, Aß-EGFP was incorporated mainly through villous columnar cells (which play a primary role in nutritional absorption) rather than through M cells (which are responsible for uptake of foreign substances) (Neutra et al., 1996). Prion protein has been thought to be selectively taken up by M cells of Peyer's patch (Heppner et al., 2002), although the possibility of incorporation of prion protein across columnar epithelial cells was recently reported (Jeffery et al., 2006). This possibility was strongly supported by the present finding of incorporation of ß-sheet proteins, such as Aß-EGFP, into columnar epithelial cells as indicated by fluorescent imaging.

The present results revealed that Aß-EGFP was mainly taken up by villous epithelial cells and moved to the interstitium. After further continuous administration, Aß-EGFP accumulated in the splenic red pulp, indicating that phagocytes which had engulfed Aß-EGFP in the enteric regions, such as Peyer's patches, where many dendritic cells are distributed (Kesall and Strober, 1996), might have transferred to the red pulp region of the spleen. This result indicates the early distribution of amyloid protein through blood circulation.

Some particles of Aß-EGFP accumulated not only in the subepithelial region of the dome epithelium in Peyer's patch, but also in the crypt interstitium. In cases of oral or intragastric challenge with scrapie pathogen in hamsters, it is thought that the infectious agent first accumulates in the Peyer's patches and then moves to the ganglia of the enteric nervous system (Beeks and McBride, 2000). The agents, therefore, may still ascend through the efferent fibers of the vagus and splanchnic nerves to finally invade the central nervous system (Beeks and McBride, 2007) (Fig. 8, red arrows). However, during suckling and weaning periods, Peyer's patches have not sufficiently developed yet. It is also reported that the distance between the regions accumulated PrP^{Sc} and peripheral nervous system is important for neuroinvasion (Prinz et al., 2003). Another route that prion protein, incorporated in villous epithelial cells or crypt patches, may directly transmit to the peripheral nervous cells without accumulation in Peyer's patches is introduced, because the peripheral nervous

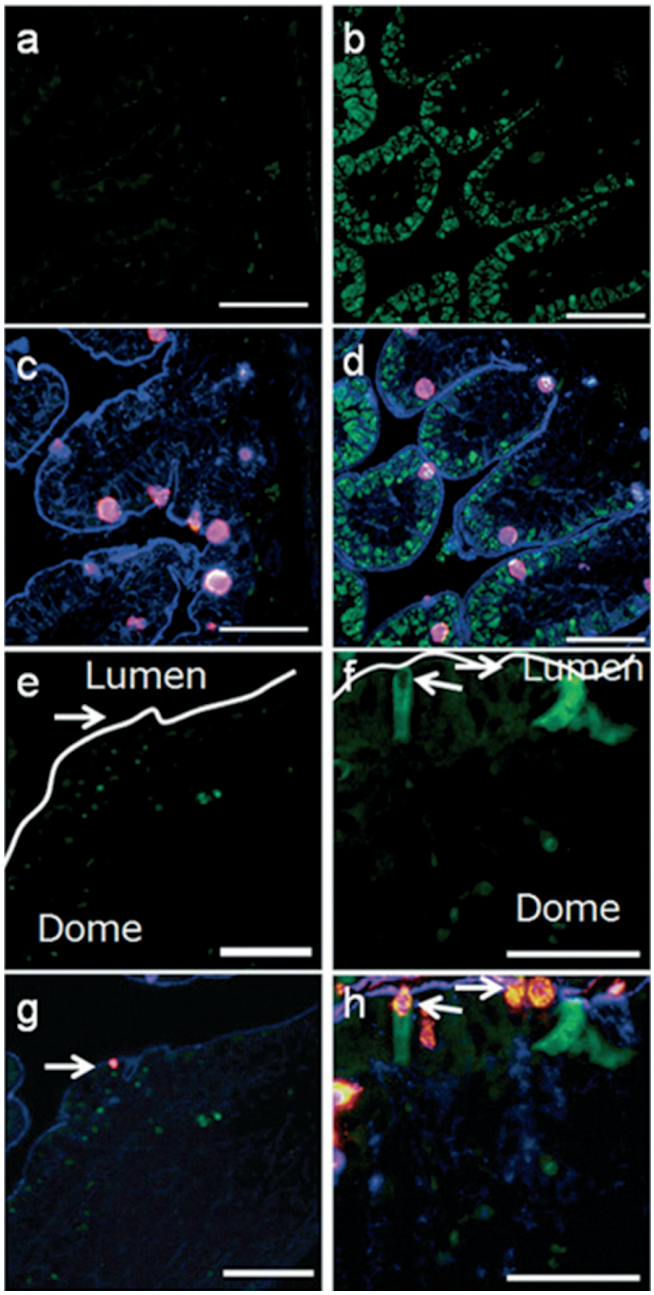

Fig. 6. Identification of cells incorporating Aß-EGFP by lectin staining. Intestinal villi **(a, b, c, d)**, Peyer's patch **(e, f, g, h)** in 10-day-old suckling mice after lectin staining. Mice were orally administered continuously with phosphate-buffered saline (PBS) **(a, c, e. g)**, Aß-EGFP **(b, d, f, h)**. Aß-EGFP was incorporated into the epithelial cells of the villus, crypt patch and Peyer's patch. PrPSc was also incorporated into the epithelial cells. Lectins used were UEA-1 conjugated with rhodamine (red) and WGA conjugated with Alexa Fluor® 350 (blue). UEA-1+/WGA- cells or M cells are indicated in red or yellow in the Peyer's patch. The luminal surface of columnar epithelial cells in the villus is shown in blue. The columnar cells and Peyer's M cells (yellow cells with arrows) engulfed Aß-EGFP (green). Scale bar: 50 μm.

cells were neighboring the incorporating regions (Fig. 8, green arrows).

The present experiment also resulted in a difference in uptake before and after weaning. The uptake of Aß-EGFP observed in suckling mice was not recognized in 25-day-old mice. Proteins such as immunogloblins and growth factors in the breast milk (Guyer et al., 1976) are incorporated into the body through the villous epithelium (Udall et al., 1981a,b; Axelsson et al., 1989) during the suckling period without losing their original

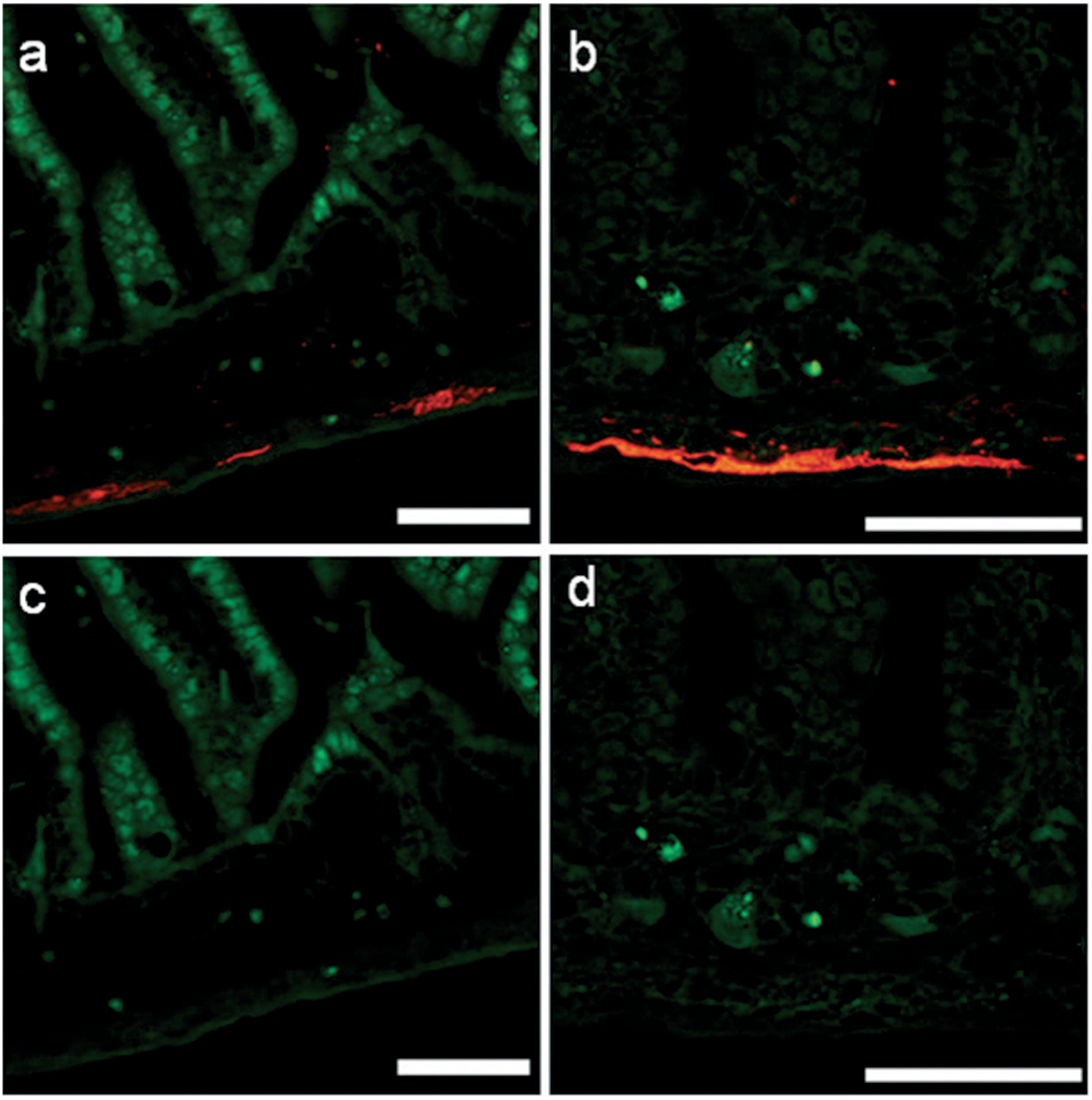

Fig. 7. Distribution of the peripheral nervous system. Intestinal villi and crypt patch. Mice were treated with conditions b **(a, c)**and d **(b, d)**. Epithelial cells incorporating Aß-EGFP and crypt patches with accumulated Aß-EGFP (green) were in close proximity to peripheral nervous cells (red). Scale bar: 50 μm.

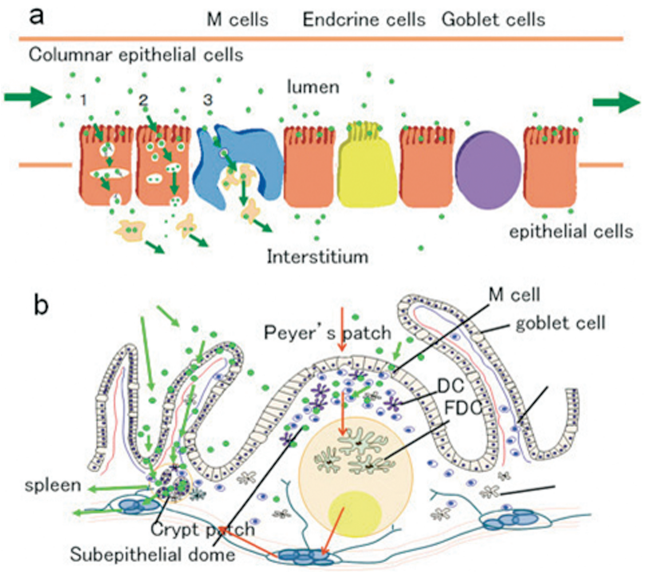

Fig. 8. The mechanism of uptake and peroral route of transmissible amyloidoses. The mechanism of Aß-EGFP uptake via the intestinal epithelium. Orally administered Aß-EGFP was incorporated mainly by columnar epithelial cells (a-1 or a-2) rather than M cells (a-3) in the villus. Aß-EGFP uptake by columnar epithelial cells may occur in specific (a-1) and nonspecific (a-2) manners. In the case of prion disease, a new pathway (green arrows) was suggested by the present experiment that differed from the conventional hypothesis (red arrows) (b).

biological activities (Chu and Walker, 1991). We previously demonstrated that the epithelium in suckling cows incorporated more foreign substances than that in weaned cow (Ano et al., 2008). In addition, during suckling periods the possibility of environmental antigenic challenge at the intestinal epithelium is lower, whereas the intestinal epithelium needs to uptake more trophic and immunomoduratory factors (Rumbo and Schiffrin, 2005). Suckling cows are thought to have the highest risk during the weaning period for infection with dietary PrP^{Sc} (Arnold and Wilesmith, 2004). Therefore, the villous epithelium at the suckling to weaning period may have a tolerant mechanism for incorporation of foreign proteins like Aß and PrP^{Sc} nonspecifically, thereby increasing the risk of transmission.

The results of the present study suggest an age-dependent mechanism for the uptake and kinetics of immediate accumulation of ß amyloid proteins within villous epithelial cells, as well as crypt and Peyer's patches, followed by further accumulation in the spleen after peroral challenge. Aß-EGFP resistance to proteases and accumulation in Peyer's patches and spleen are common in cases of prion disease.

Acknowledgements. This work was supported by a Grant-in-Aid from the Food Safety Commission in the Japanese Government Cabinet Office.

References

Ano Y., Nakayama H., Sakai Y., Sakudo A., Endo M., Ebisu S., Li J.Y., Uetsuka K., Manabe N. and Onodera T. (2008) Incorporation of ,-amyloid protein through the bovine ileal epithelium before and after weaning: Model for orally transmitted amyloidoses. Microbiol. Immunol. 52, 429-434.

Arnold M.E. and Wilesmith J.W. (2004). Estimation of the age-dependent risk of infection to BSE of dairy cattle in Great Britain. Prev. Vet. Med. 66, 35-47.

Axelsson L., Jakobsson L., Lindberg T., Poleberger S., Benediktsson B. and Raiha N. (1989) Macromolecular absorption in preterm and term infant. Acta. Paediatr. Scand. 78, 532-537.

Beeks M. and McBride P.A. (2000). Early accumulation of pathological PrP in the enteric nervous system and gut-associated lymphoid tissue of hamster orally infected with scrapie. Neurosci. Lett. 278, 181-184.

Beeks M. and McBride P.A. (2007). The spread of prions through the body in naturally acquired transmissible spongiform encephalopathies. FEBS J. 274, 588-605.

Bradley M.S. and Nishikida K.. (2005). Infrared Measurement of proteins: Theory and Applications. Thermo Fischer Scientific. Madison

Chu S.H. and Walker W.A. (1991). Growth factor signal transduction in human intestinal cells. Adv. Exp. Med. Biol. 310, 107-112.

Clark M.A., Jepson M.A., Simmons N.L., Booth T.A. and Hirst B.H. (1993). Differential expression of lectin-binding sites defines mouse intestinal M-cells. J. Histochem. Cytochem. 41, 1679-1687.

Cui D., Kawano H., Takahashi M., Hoshi Y., Setoguchi M., Gondo T. and Ishihara T. (2002). Acceleration of murine AA amyloidosis by oral administration of amyloid fibrils extracted from different species. Pathol. Int. 52, 40-45.

Guyer R.L., Koshland M.E. and Knopf P.M. (1976). Immunoblobluin binding by mouse intestinal epithelial cell receptors. J. Immunol. 117, 587-593.

Heppner F.L., Christ A.D., Klein M.A., Prinz M., Fried M., Kraehenbuhl J.P. and Aguzzi A. (2002). Transepithelial prion transport by M cells. Nat. Med. 7, 976-977.

Hering J.A., Innocent P.R. and Haris P.I. (2002). Automatic amide I frequency selection for rapid quantification of protein secondary structure from Fourier transform infrared spectra of proteins. Proteomics 2, 839-849.

Hunyady B., Mezey E. and Palkovits M. (2002). Gastrointestinal immunology: cell types in the lamina propria a morphological review. Acta. Physiol. Hung. 87, 305-328.

Jeffery M., Gonzales L., Espenes A., Press C.M., Martin S., Chaplin M., Davis L., Landsverk T., MacAldowie C., Eaton S. and McGovern G. (2006). Transportation of prion protein across the intestinal mucosa of scrapie-susceptible and scrapie-resistant sheep. J. Pathol. 2006, 209:4-14.

Johan K., Westermark G., Engstorm U., Gustavsson A., Hultman P. and Westermark P. (1998). Acceleration of amylioid protein A amyloidosis by amyloid-like synthetic fibrils. Proc. Natl. Acad. Sci. 95, 2558-2563.

Kelsall B.L. and Strober W. (1996). Distinct populations of dendritic cells are present in the subepithelial dome and T cell regions of the murine Peyer's patch. J. Exp. Med. 183, 237-247.

Melanie M.L. and Mathias J. (2006). Exogenous induction of cerebral ß-amyloisosis is governed by agent and host. Science 313, 1781-

1784.

Neutra M.R., Phillips T.L., Mayer E.L. and Fishkind D.J. (1996). Epithelial M cells: gateways for mucosal infection and immunization. Cell 8, 345-348.

Prinz M., Heikenwalder M., Junt T., Schwarz P., Glatzel M., Heppner F.L., Fu Y.X., Lipp M. and Aguzzi A. (2003). Positioning of follicular dendritic cells within the spleen controls prion neuroinvasion. Nature 425, 957-962.

Riek R. (2006). Infectious Alzheimer's disease. Nature 444, 429-430.

Rumbo M. and Schiffrin E.J. (2005). Ontogeny of intestinal epithelium immune functions: developmental and environmental regulation. Cell. Mol. Life Sci. 62, 1288-1296.

Udall J.N., Colony P., Fritze L., Pang K., Trier J.S. and Walker W.A. (1981a). Development of gastrointestinal mucosal barrier: The effect of natural versus artificial feeding on intestinal permeability to macromolecules. Pediatr. Res. 15, 245-249.

Udall J.N., Pang K., Fritze L., Kleinman R. and Walker W.A. (1981b). Development of gastrointestinal mucosal barrier: The effect of age on intestinal permeability to macromolecules Pediatr. Res. 15, 241-244.

Westermark P. (1998). The pathogenesis of amyloidosis: Understanding general principles. Am. J. Pathol. 152, 1125-1127.

Xing Y. and Higuchi K. (2001). Transmission of mouse senile amyloidosis. Lab. Invest. 81, 493-499.

Xing Y. and Higuchi K. (2002). Amyloid fibril proteins. Mech. Ageing Dev. 123, 1625-1636.

Accepted September 29, 2008